

# Study and Analysis on a High-Frequency Current-Source Single-Stage PFC Converter\*

Jindong Zhang and Fred C. Lee

Center for Power Electronic Systems  
The Bradley Department of Electrical Engineering  
Virginia Polytechnic Institute and State University  
Blacksburg, VA 24061-0111  
Email: [henry@vpec.vt.edu](mailto:henry@vpec.vt.edu)

Milan M. Jovanović

Delta Products Corporation  
Power Electronics Laboratory  
P. O. Box 12173  
5101 Davis Drive  
Research Triangle Park, NC 27709

## ABSTRACT

The study and analysis of a high-frequency current-source (CS) single-stage power-factor-correction (S<sup>2</sup>PFC) converter is presented in this paper. The general principles of the S<sup>2</sup>PFC techniques are introduced first. Based on the general principles, this paper focuses on the CS S<sup>2</sup>PFC technique and explores the effects of different circuit parameters on the input current THD and current ripple, the switch current stress, the energy-storage capacitor voltage stress and the overall efficiency. Simulation and experimental data are given to support the study and analysis.

## I. INTRODUCTION

In recent years, many single-stage power factor correction (S<sup>2</sup>PFC) techniques have been proposed to comply with IEC 1000-3-2 input current harmonics limits with low-cost and good performance. The input boost inductor in a S<sup>2</sup>PFC converter can be operated in either discontinuous-conduction-mode (DCM) or continuous-conduction-mode (CCM). Generally, CCM S<sup>2</sup>PFC converters are more desirable because of their small EMI filter, low current stress and good efficiency.

Figure 1 shows two CCM S<sup>2</sup>PFC circuits with an additional high-frequency inductor  $L_1$  [1][2]. Though these two circuits have different circuit topologies, they are functionally equivalent circuits. As a simple case, these two converters can be operated while  $N_1=N_p$  in Fig. 1(a) or no tapping on  $N_p$  in Fig. 1(b). In this case, the ideal waveforms of input voltage and boost inductor current are shown in Fig. 2. Because the high-frequency inductor  $L_1$  can be regarded as a high-frequency current source, in this paper, the circuits in Fig. 1 are called current-source (CS) CCM S<sup>2</sup>PFC circuits.

Above CS S<sup>2</sup>PFC converters have good performance and low cost. Therefore, they have been proposed and studied in [1-4]. However, further study is still necessary to provide a comprehensive understanding and detailed design considerations of this converter. This paper focuses on the CS S<sup>2</sup>PFC converter and explores the effects of different circuit parameters on the input current THD and current ripple, the switch current stress, the energy-storage capacitor voltage stress, and overall efficiency. Simulation and experimental data are given to support the study and analysis.

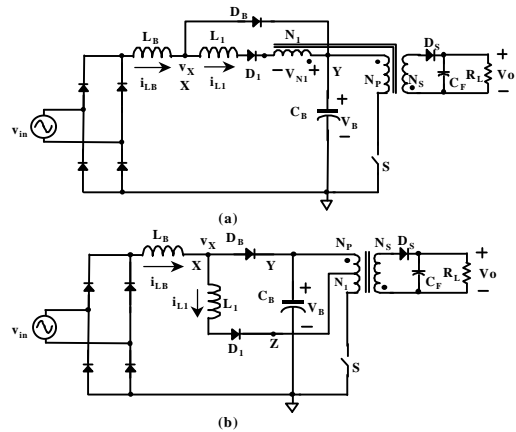


Fig. 1 CCM current-source S<sup>2</sup>PFC circuits with: (a) two-terminal cell [2]; (b) three terminal cell [1]

## II. BRIEF EXPLANATION OF THE PFC FUNCTION OF THE CS S<sup>2</sup>PFC CONVERTER

As shown in Fig. 2, in order to achieve perfect input current shaping in the conventional CCM boost PFC converter, the switch duty cycle  $d_{PFC}$  has to decrease with the instantaneous line voltage increase in each half line cycle. Equation (1) shows the required duty-cycle of the CCM boost PFC converter during a half-line cycle[4]:

$$d_{PFC}(t) = 1 - \frac{V_{in(peak)} \cdot |\sin \omega t|}{V_B} \quad (1)$$

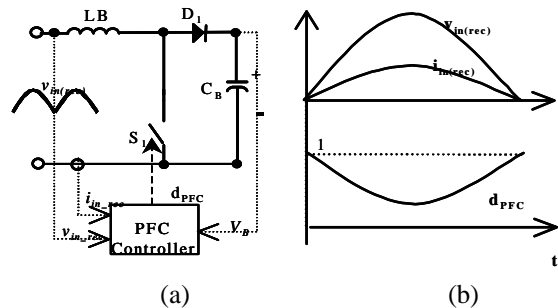


Fig. 2 Ideal CCM boost PFC circuit and its waveforms: (a) Circuit diagram, and, (b) ideal voltage, current and duty-cycle waveform during a half line cycle

\* This work was supported in part by a fellowship from Delta Electronics, Inc. This work made use of ERC Shared Facilities supported by the U.S. National Science Foundation under Award Number EEC-9731677.

However, in an integrated S<sup>2</sup>PFC converter, the switch duty cycle is almost constant during a line cycle if the DC/DC stage is already in the steady state. To achieve input-current-shaping on a CCM S<sup>2</sup>PFC boost inductor, the effective duty-cycle on the S<sup>2</sup>PFC boost inductor should be modulated in the way similar to the ideal PFC duty-cycle shown in Fig. 2(b). In the CS S<sup>2</sup>PFC converter, the effective duty-cycle is achieved by the additional current-source inductor L<sub>1</sub>. Figure 3 shows the input current waveforms of the CS S<sup>2</sup>PFC converter and Fig. 4 shows the principle switching waveforms of the CS S<sup>2</sup>PFC converters at different time instances A and B in Fig.3. Because the current commutation between the boost diode D<sub>B</sub> and the CS inductor L<sub>1</sub> after switch S is turned on in each switching cycle [3], the effective duty-cycle on the boost inductor is actually less than the switch duty-cycle D, as shown in Fig. 4. Fig. 4 also shows that the instantaneous effective duty-cycle D<sub>eff</sub> decreases with the line voltage increases, which follows the shape of the ideal PFC duty cycle in Fig. 2(b). Equation (2) represents the effective duty cycle D<sub>eff</sub>. When the input voltage rises, the boost inductor current i<sub>LB</sub> also rises. As the result, the effective duty cycle will decrease. Therefore, the input current can be shaped.

Above is just a brief explanation of the principle of the CCM CS S<sup>2</sup>PFC circuits. In following sections, the detailed discussions on the effects of several key parameters will be given and a design guideline will be provided.

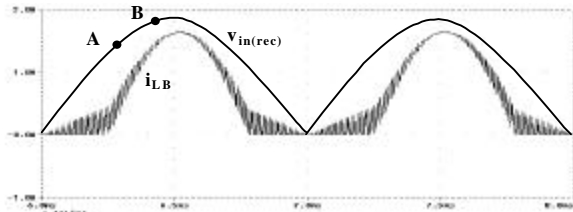


Fig. 3 Line cycle waveforms of CS S<sup>2</sup>PFC circuit

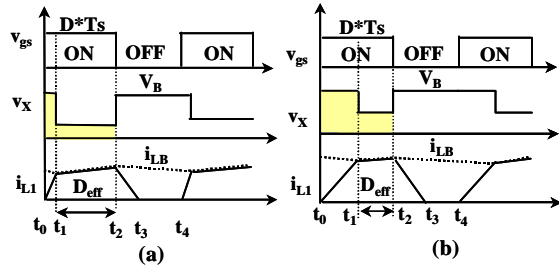


Fig. 4 Switching waveforms of the CS S<sup>2</sup>PFC circuit

$$D_{eff} = \frac{DV_B - L_1 f_s i_{LB}}{V_B - \frac{v_{in(rec)} \cdot L_1}{L_1 + L_B}} \approx D - \frac{L_1 \cdot f_s \cdot i_{LB}}{V_B} \quad (2)$$

(Only apply to L<sub>B</sub> in CCM mode)

### III. STUDY AND DISCUSSIONS OF THE CS S<sup>2</sup>PFC CONVERTERS

In order to provide design guidelines to help further understand and optimize the CS S<sup>2</sup>PFC circuit, further study is necessary. In this section, the analysis and design guidelines will be discussed on different circuit parameters and different issues.

#### 3.1 INPUT CURRENT HARMONICS

According to the input-current-shaping (ICS) mechanism of the CS S<sup>2</sup>PFC converter, theoretically, L<sub>1</sub> is the key design parameter for input current harmonics. To get adequate input current harmonics margin to meet the IEC61000 harmonics standard, L<sub>1</sub> need be operated in DCM mode. Therefore, each switching cycle when the switch is turn on, the current in L<sub>1</sub> can start from zero to get a strong modulation effect. Similarly, from the modulation effect point of view, a large L<sub>1</sub> is preferred. However, L<sub>1</sub> cannot be too large, otherwise L<sub>1</sub> will enter CCM mode at low line, full load. If so, as can be seen in Fig. 5, the time interval t<sub>0</sub>-t<sub>1</sub> for L<sub>1</sub> current to reach i<sub>LB</sub> will be reduced because the initial value of i<sub>L1</sub> is larger than zero. Figure 5(a) shows L<sub>1</sub> in DCM with strong effect on duty-cycle while fig. 5(b) shows L<sub>1</sub> in CCM with reduced effect on duty cycle. Consequently, the PFC modulation effect will be hurt if L<sub>1</sub> enters CCM mode.

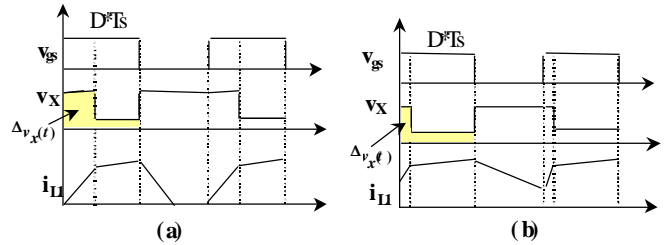


Fig. 5 Over-designed L<sub>1</sub> will enter CCM current mode  
(a) Switching waveform with properly designed DCM L<sub>1</sub>  
(b) Switching waveform with over-designed L<sub>1</sub>

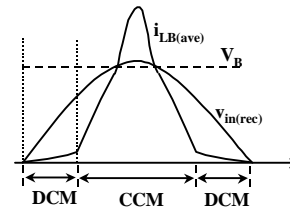


Fig. 6 Conceptual waveform of high current distortion caused by over-designed L<sub>1</sub> while V<sub>B</sub> is already lower than v<sub>in(peak)</sub>

Besides, it is necessary to point out that there is another big impact if L<sub>1</sub> is over-designed. Because L<sub>1</sub> can reduce the effective duty-cycle on the boost inductor, it also reduces the bulk-capacitor voltage V<sub>B</sub>. If L<sub>1</sub> is too large, V<sub>B</sub> will be too low so that it can be even lower than the peak input voltage.

As the result,  $L_B$  cannot have adequate reset during the time interval while  $v_{in(rec)}$  is higher than  $V_B$ .  $L_B$  will be saturated and have a highly distorted current peak, as shown in Fig. 6.

As a summary, to satisfy the PFC condition a large  $L_1$  is preferred but  $L_1$  cannot be too large. In section 4, a design curve of  $L_1$  will be given.

### 3.2 BULK CAPACITOR VOLTAGE STRESS

The bulk energy-storage capacitor voltage  $V_B$  stress in a  $S^2PFC$  converter is also a key design consideration. In the ideal CCM boost PFC converter, the boost output voltage is given in Equation 3, which shows the relationship between half-line-average duty-cycle  $D_{AVE}$  and boost output voltage  $V_B$ . The CS CCM  $S^2PFC$  converter has much lower voltage stress than the DCM  $S^2PFC$  converter without capacitor voltage-feedback windings. This can be explained with two reasons. First, the CS  $S^2PFC$  converter is designed to have CCM boost inductor current. This means that  $L_B$  in the CS  $S^2PFC$  converter has much larger inductance than it does in a DCM  $S^2PFC$  converter. Normally, in  $S^2PFC$  converter, a large boost inductor  $L_B$  helps to reduce  $V_B$  stress [6]. However, the more important reason is that the additional inductor  $L_1$  introduces effective boost duty-cycle  $D_{eff}$  on  $L_B$  and  $D_{eff}$  is smaller than the switch duty-cycle. With the reduced duty-cycle, capacitor voltage  $V_B$  is reduced. In the CS  $S^2PFC$ , theoretically, the boost capacitor voltage  $V_B$  should be able to be calculated in a similar way as in Equation 3 while the  $D_{AVE}$  is actually the average of the effective duty-cycle  $D_{eff}$ . However, because the switch duty-cycle is determined by the dc/dc output stage and  $V_B$  changes with load and line changes, an numerical integration has to be used based on the input/output power balance, in order to calculate the actual  $V_B$  in stead of a simple equation like Equation 3.

$$V_B = \frac{V_{in(AVE)}}{1 - D_{AVE}} \quad (3)$$

--- (Use  $D_{eff(AVE)}$  if in CCM  $S^2PFC$  circuit)

Nevertheless, Equation 2 and 3 can conceptually show how the  $V_B$  changes with the load current or  $L_1$ . If output load current decreases, the input inductor current  $i_{LB}$  will also decrease to maintain the input/output power balance. According to Equation 2, the effective duty-cycle will increase. Therefore, the capacitor voltage  $V_B$  will increase at light load. On the other hand, large  $L_1$  will always give smaller effective duty-cycle, resulting in lower  $V_B$ . To provide adequate voltage margin for the 450 V electrolytic capacitor at high line, light load, a large  $L_1$  is always preferred to further reduce  $V_{B(max)}$ , as long as  $V_B$  is higher than the minimum  $V_{in(peak)}$  at low line, full load.

Other than using a large  $L_1$ , there is a more effective way to reduce  $V_B$  stress [1][3]. It is to use a tapped dc/dc converter transformer as shown in Fig. 1(b) or design the winding  $N_1$  to be less than  $N_p$  as in Fig.1 (a). The principle of the tapped transformer is similar as the DCM  $S^2PFC$  converter with feedback winding  $N_1$  [6]. Generally, with the feedback winding or transformer tapping,  $V_B$  stress can be reduced significantly and the efficiency can be improved. Besides, in the CS  $S^2PFC$  converter, the feedback winding can reduce the voltage-second on  $L_B$  and  $L_1$ , therefore, smaller cores may be used to reduce the size and cost. The effect of feedback winding can be quantified by the feedback ratio  $K_{FB}$ , which is defined as in Equation 4 or 5 for the  $S^2PFC$  circuits in Fig. 2(a) or 2(b), respectively. Once these two circuits have same feedback ratio  $K_{FB}$ , they have identical functionality and performance.

$$\text{In two-terminal } S^2PFC: K_{FB} = \frac{N_p - N_1}{N_p} \quad (4)$$

$$\text{In three-terminal } S^2PFC: K_{FB} = \frac{N_1}{N_p} \quad (5)$$

The drawback of using a feedback winding or transformer tapping is the dead conduction angle on the input current introduced by the winding  $N_1$  [3][6]. With the induced voltage on winding  $N_1$  in Fig. 2(b), the front-end diode-bridge can not have input current near the line-voltage-crossover time interval. The dead conduction angle will cause additional input current distortion. Nevertheless, it is necessary to point out that for low power application ( $P_{in} < 600W$ ) in IEC61000 class D range, it is fine for the input current have certain distortion. In fact, minimum current distortion is not a design goal as long as the current harmonics can meet IEC limits [6]. An optimized circuit should have the input current harmonics just lower than the IEC limits with certain margin, and, have optimized efficiency, low voltage stress and low cost.

As a summary, from reducing  $V_B$  stress point of view, an optimal design needs  $L_1$  and  $N_1/N_p$  to be as large as possible while the input current can still meet IEC harmonics limits. A design approach will be presented in section 4 with experimental data.

### 3.3 CURRENT STRESS AND EFFICIENCY

The converter efficiency is also an important consideration of the  $S^2PFC$  converters. To get good efficiency, there are two major design parameters to be considered. As discussed in previous section, the current-source inductor  $L_1$  and transformer tapping  $N_1/N_p$  (Fig. 2(b)) can reduce the bulk capacitor voltage stress. A lower  $V_B$  means lower rating semiconductor component and lower semiconductor loss. Furthermore, as can be seen on Fig. 7,

a large  $L_1$  or a higher  $N_1/N_p$  ratio can reduce the charging rate of the inductor current  $i_{L1}$  after switch  $S$  is turned on at  $t_0$ . In Fig. 7, the dashed line shows the  $v_X$  and  $i_{L1}$  waveforms with a smaller  $L_1$  or  $N_1/N_p$  and the solid line shows the  $v_X$  and  $i_{L1}$  waveforms with a larger  $L_1$  or  $N_1/N_p$ . As can be seen, the RMS current through  $L_1$  to switch  $S$  can be reduced with large  $L_1$  value or high  $N_1/N_p$  ratio. Therefore, the switch conduction loss can be reduced. As a result, large  $L_1$  or high  $N_1/N_p$  ratio can improve the converter efficiency. This is proved experimentally in section 4. Again, as discussed in previous sections, the value of  $L_1$  or  $N_1$  cannot be too high because of the constraint from the input current harmonics limits.

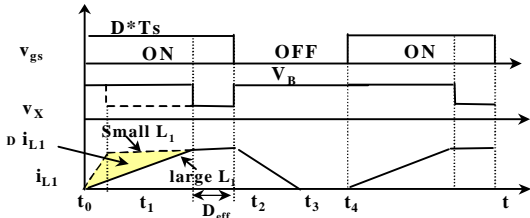


Fig. 7 Reduced switch current with  $L_1$  or  $N_1/N_p$  (Fig.2(b))

#### IV. SIMULATION AND EXPERIMENTAL DESIGN STUDY OF THE CS S<sup>2</sup>PFC CONVERTER

Different  $L_B$  and  $L_1$  values have been studied with simulation and experiment for the design optimizations. The simulation/experimental circuit is designed to have a universal-line input (90-265Vac) and 5V/40A output, which is similar to the specifications of a typical low-end computer power supply. One fundamental problem for the circuits in Fig. 2 are their wide capacitor voltage  $V_B$  range with universal line input [7]. To optimize the performance in universal-line range, the voltage-doubler version of CS S<sup>2</sup>PFC circuit [8] has to be used as shown in Fig. 8. The voltage-doubler CS S<sup>2</sup>PFC circuit has same operation principle as the circuit in Fig. 2 except there is a range-selection switch  $SW$ , which is always closed in the American line range (90-135V<sub>ac</sub>) and opened in the European line range (180-265V<sub>ac</sub>).

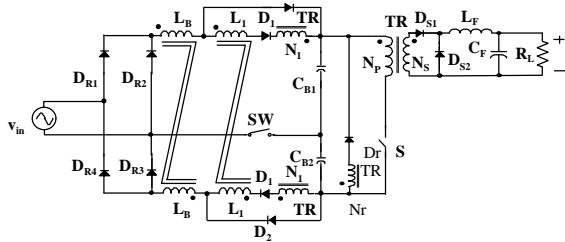


Fig. 8 Circuit diagram for simulation and experiment

The key experimental circuit components have been chosen as follows:  $L_B$ : 45 - 190  $\mu\text{H}$ ,  $L_1$ : 30 -

100  $\mu\text{H}$  (each winding),  $N_1 = 14$  T,  $N_p = 52$  T,  $N_r = 52$  T and  $N_s = 3$  T,  $C_{B1,2}$ : 470  $\mu\text{F}/250\text{V}$ , switch  $S$ : IXYS 12N100 and Schottky diode  $D_{S1-2}$ : IR81CND45, switching frequency  $f_s=70\text{kHz}$ . It is necessary to point out that the feedback ratio  $K_{FB}$  for this voltage-doubler S<sup>2</sup>PFC should be defined in Equation 7 to have same effect as  $K_{FB}$  in the CS S<sup>2</sup>PFC circuit in Fig. 2(a).

$$K_{FB} = \frac{0.5 \cdot N_p - N_1}{0.5 \cdot N_p} \quad (7)$$

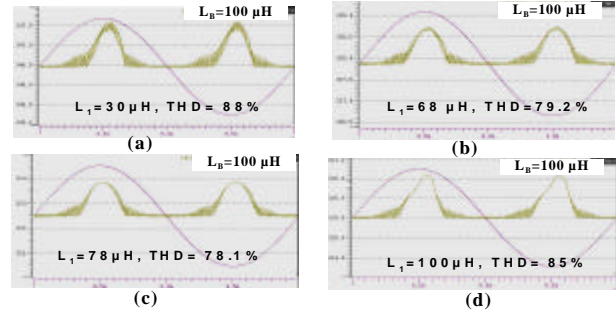


Fig. 9 Different boost inductor current with different  $L_1$

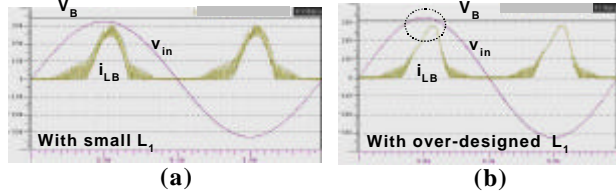


Fig.10 Simulation waveforms show low  $V_B$  cause  $i_{LB}$  distortion with over-designed  $L_1$

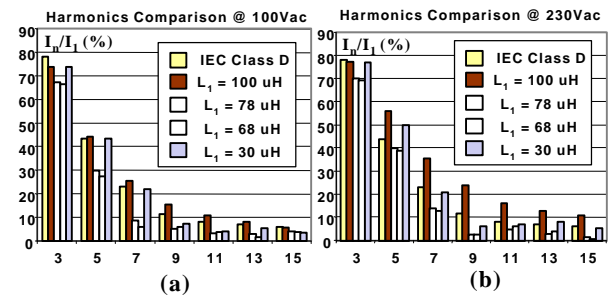


Fig. 11 Line input current harmonics with different  $L_1$

First, to study the  $L_1$  effect on the input current,  $L_B$  was fixed at 100  $\mu\text{H}$  and several different  $L_1$  have been used in the circuit in Fig. 8. Figure 9 shows different input current waveforms in simulations with different  $L_1$  inductance at 230 V<sub>ac</sub>, full load. This figure was obtained with a closed voltage-loop simulation with Simplis® software. As shown in Figure 9(d), if  $L_1$  is over designed, there is high distortion on the input current because  $V_B$  is lower than  $V_{in(peak)}$ . The input current THD is about 85%. After  $L_1$  was decreased to 78  $\mu\text{H}$ ,

$V_B$  was already higher than  $v_{in(peak)}$ . Therefore, the input current has much less distortion and input current THD was reduced to 78.1%, as shown in Fig. 9(c). After that, if  $L_1$  was too small, the converter did not have enough PFC modulation and the distortion increased again. For example, as shown in Fig. 9(a), input current has high distortion again and THD = 88%. Figure 10 shows the simulation waveforms with properly-designed  $L_1$  and over-designed  $L_1$ . It confirms that with over-designed  $L_1$ ,  $V_B$  will be lower than  $V_{in(peak)}$ , resulting in high current distortion. Figure 11 shows the current harmonics comparison with different  $L_1$ . As can be seen, for  $L_1$  around 68 and 78  $\mu\text{H}$ , the CS  $S^2\text{PFC}$  circuit can meet the IEC standard with plenty margin.

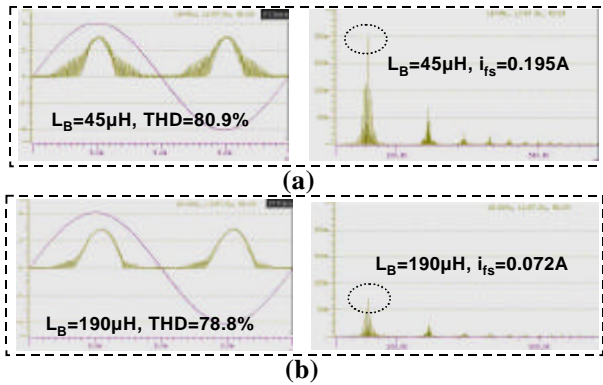


Fig. 11 Boost inductor current waveforms with different  $L_B$

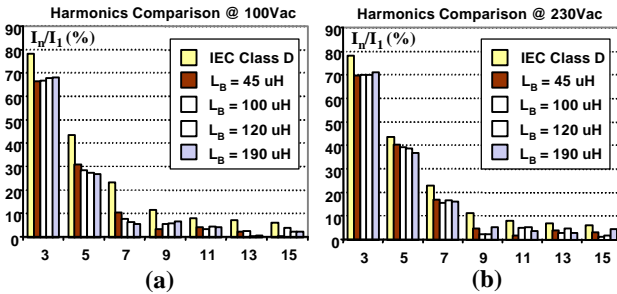


Fig. 12 Line input current harmonics with different  $L_B$

To show  $L_B$ 's effect on the input current,  $L_1$  is fixed as  $L_1=68 \mu\text{H}$  and several different  $L_B$  values were used in the experimental circuit. Figure 11 shows the different boost inductor current waveforms in simulations and the input current THD. As can be seen, the input current THD just changed a little while  $L_B$  had significantly different values, from 45  $\mu\text{H}$  to 190  $\mu\text{H}$ . It shows that  $L_B$  has relatively weak effect on the low frequency input current harmonics. This fact is also proved by Fig. 12, which shows the low frequency input current harmonics with different  $L_B$ . However, as shown in Fig. 11, the effect of different  $L_B$  is the difference on the boost inductor current ripple at switching frequency. A large  $L_B$  means small current ripple on  $L_B$ . Theoretically, the current ripple should be determined by the total inductance  $L_B + L_1$ . This is because during the time interval of boost

inductor charging, these two inductors have the total input voltage on them. Figure 13 shows the curve of total inductance vs. the boost current ripple. The switching frequency current ripple is going to determine the differential mode EMI filter size.

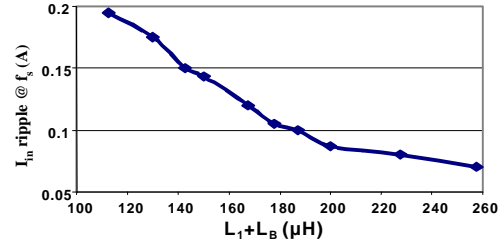


Fig. 13 Switching-frequency current ripple on boost inductor is determined by the total inductance of  $L_B$  and  $L_1$

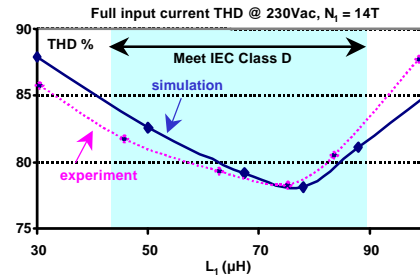


Fig. 14 Simulated and experimental  $L_1$  vs. THD curve

$$\text{Normalized } L_1: L_1^* = L_1 \cdot f_s \cdot P_o / h \quad (8)$$

Figure 14 provides the simulation and experiment curves of the input current THD vs.  $L_1$ . It shows the simulation result is quite close to the experimental result. This curve can be used for design reference of the CS  $S^2\text{PFC}$  with fixed feedback ratio  $K_{FB} = 0.4 \sim 0.5$ . It is necessary to point out that this  $K_{FB}$  is already close to optimized value for universal line input, based on our experience. In a design,  $L_1$  should be chosen inside the shaded area to guarantee the input current harmonics meet IEC class D limits. Generally, within this shaded area in Fig. 14,  $L_1$  should be chosen as large as possible to get the low  $V_B$  stress and the good efficiency. For the circuit with different output power  $P_o$ , efficiency  $\eta$  and switching frequency  $f_s$ , the curve shown in Fig. 14 can be normalized with Equation 8. The principle of normalization is based on the effective duty-cycle  $d_{eff}$  by Equation 2.

Figure 15 shows  $L_B$ 's and  $L_1$ 's effects on the bulk capacitor voltage  $V_B$  stress in the experiment. As can be seen, a larger  $L_B$  or  $L_1$  will result in a lower  $V_B$ . Figure 16 shows different measured efficiencies with different  $L_B$  and  $L_1$ . As can be seen in Fig. 16(a), a large  $L_B$  can increase efficiency a little (less than 0.4%) because of smaller current ripple. On the other hand,  $L_1$  has stronger effect on the

efficiency (about 2.6% difference). By increasing  $L_1$  value, as discussed in Section 3, the switch current stress can be reduced and a better efficiency can be achieved. However, after  $L_1$  reaches a certain value, because  $V_B$  starts to be lower than  $V_{in(peak)}$ , a high current peak occurs which increase the current stress. The efficiency does not increase any longer. With the voltage-doubler front-end, the full-load (5V/40A) efficiency of this converter is higher than 80% in full line range (90-265Vac) which is better, or, at least comparable to two-stage PFC approach.

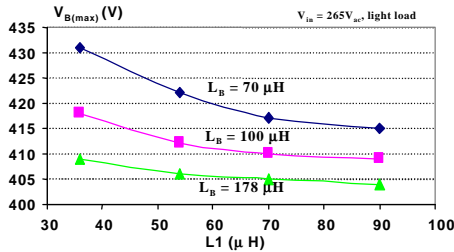


Fig. 15 Capacitor voltage  $V_{B(max)}$  changes with  $L_1$  and  $L_B$

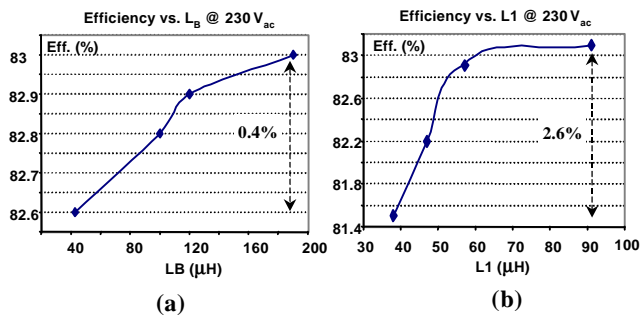


Fig. 16 Full load efficiency with different  $L_1$  and  $L_B$

In summary, many different issues need to be considered during the design of this converter. The feedback winding ratio  $K_{FB}$  with  $N_1$ , inductor  $L_B$  and  $L_1$  are important design parameters of the CS  $S^2$ PFC converter. Generally, as to  $N_1$ , the feedback ratio  $K_{FB}$  should be chosen as high as possible to achieve high efficiency and low  $V_B$  stress, until it is hard for the converter to meet IEC61000 Class D harmonics limits. The optimized  $K_{FB}$  is in 0.4~0.5 range.  $L_1$  and  $L_B$  should be selected by considering Figs. 14 – 16. The design objective is to get the lowest  $V_B$  stress and highest efficiency while the converter can still meet IEC harmonics limits. Within the IEC limits,  $L_1$  should be chosen a large value based on Fig. 14. To provide a straightforward design approach, Fig. 17 summarizes the design steps and provides clear design guidelines of the voltage-doubler CCM CS  $S^2$ PFC for universal line applications. It is necessary to point out that a few straightforward steps are not enough for the design optimization of this converter. Numerical analysis, simulations, and experiments are all necessary to get the optimal design. In addition, the dc/dc output stage design should be quite similar as the conventional dc/dc converter design.

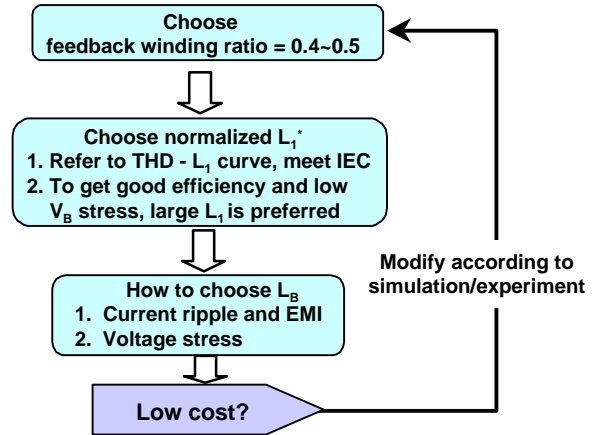


Fig. 17 Design guideline of CS  $S^2$ PFC converter (with voltage-doubler front-end for universal line input)

## V. SUMMARY

In this paper, the detailed analysis and experimental data have been provided to explore the issues in the CCM CS  $S^2$ PFC converter. Different circuit parameters' effect on input current, switch current stress, circuit voltage stress and overall efficiency have been presented. Design considerations and guidelines have been discussed with the simulation and experimental data.

## REFERENCES

- G. C. Hua, "Consolidated Soft-Switching AC/DC Converters," U.S. Patent NO. 5,790,389, Aug. 4, 1998.
- J. Sebastian, M.M. Hernando, P. Villegas, J. Diaz, A. Fontan, "Input Current Shaper Based on The Series Connection of A Voltage Source and A Loss-Free Resistor," *IEEE Applied Power Electronics Conf. (APEC) Proc.* 1998, pp. 461-467
- L. Huber and M.M. Jovanovic, "Design optimization of single-stage, single-switch input-current shapers," *IEEE Power Electronics Specialists Conf. (PESC) Record*, 1997, pp.519-526.
- J. Zhang, M.M. Jovanovic, and F. C. Lee, "General Studies on Single-Stage Power-Factor-Correction Techniques", *17<sup>th</sup> Virginia Tech Power Electronics Seminar Proc.*, Sept. 1999
- F.S. Tsai, et al, "Low Cost AC-to-DC Converter Having Input Current with Reduced Harmonics," U.S. Patent No. 5,652,700, Jul. 29, 1997.
- Q. Zhao, F. C. Lee, and F. Tsai, "Design Optimization of an Off-Line Input Harmonic Current Corrected Flyback Converter," *IEEE Applied Power Electronics Conf. (APEC) Proc.* 1999, pp 91-97
- J. Zhang, M.M. Jovanovic, and F. C. Lee, "Comparison between CCM two-stage and single-stage boost PFC converters," *IEEE Applied Power Electronics Conf. (APEC) Proc.* 1999, pp 335 – 310.
- J. Zhang, L. Huber, M. M. Jovanovic, and F.C. Lee, "Single-Stage Input Current Shaping Techniques with Voltage-Doubler-Rectifier Front End", *IEEE Applied Power Electronics Conference (APEC) Proc.*, Mar. 1999, pp 112 - 118